

Nova Sagittarii 1998 (V4633 Sgr): a permanent superhump system or an asynchronous polar?

Y. Lipkin,^{1★} E. M. Leibowitz,^{1★} A. Retter^{2,3★} and O. Shemmer^{1★}

¹School of Physics and Astronomy, and the Wise Observatory, Raymond and Beverly Sackler Faculty of Exact Sciences, Tel-Aviv University, Tel Aviv 69978, Israel

²Department of Physics, Keele University, Keele, Staffordshire ST5 5BG

³School of Physics, University of Sydney, 2006, Australia

Accepted 2001 August 23. Received 2001 July 11; in original form 2001 February 15

ABSTRACT

We report the results of observations of V4633 Sgr (Nova Sagittarii 1998) during 1998–2000. Two photometric periodicities were present in the light curve during the three years of observations: a stable one at $P = 3.014$ h, which is probably the orbital period of the underlying binary system; and a second one of lower coherence, approximately 2.5 per cent longer than the former. The latter periodicity may be a permanent superhump, or, alternatively, the spin period of the white dwarf in a nearly synchronous magnetic system. A third period, at $P = 5.06$ d, corresponding to the beat between the two periods was probably present in 1999. Our results suggest that a process of mass transfer has taken place in the binary system since no later than two-and-a-half months after the nova eruption. We derive an interstellar reddening of $E(B - V) \sim 0.21$ from our spectroscopic measurements and published photometric data, and estimate a distance of $d \sim 9$ kpc to this nova.

Key words: accretion, accretion discs – stars: individual: V4633 Sgr – novae, cataclysmic variables.

1 INTRODUCTION

Nova Sagittarii 1998 (V4633 Sgr) was discovered on 1998 March 22 by Liller (1998). Brightest visual magnitude of 7.4 mag was reported by Jones (1998) on March 23.7. Liller & Jones (1999) classified V4633 Sgr as a fast nova, with $t_3 \approx 35$ d for the visual observations, and ≈ 48 d in charge-coupled device (CCD) broadband V. An early spectrum of V4633 Sgr revealed slow expansion velocities and massive presence of iron, implying a Fe II classification (Della Valle, Pizzella & Bernardi 1998).

Skiff (1998) reported no definite object at the location of V4633 Sgr in the Palomar Sky Survey, setting a lower limit of 12 mag on the outburst amplitude.

Spectropolarimetry of V4633 Sgr shortly after maximum brightness did not yield evidence for intrinsic polarization (Ikeda, Kawabata & Akitaya 2000).

Infrared spectrophotometry indicated that V4633 Sgr was in the early stages of its coronal phase in 1999 August (Rudy et al. 1999), and revealed strong coronal lines, and a relatively low reddening in 2000 July (Rudy et al. 2000).

Lipkin, Retter & Leibowitz (1998) reported a photometric

modulation in the light curve (LC) of V4633 Sgr, with a period of 0.17330 or 0.14765 ± 0.00011 d, which are 1-d aliases of each other. The modulation was detected eleven weeks, and possibly as early as six weeks, after the eruption. Later on, Lipkin & Leibowitz (2000) found that another 1-d alias, at 0.128 791 d, is in fact the dominant periodicity in the LC. They also reported the discovery of a second photometric periodicity at 0.125 573 d, modulating the brightness of the star along with the first one during 1999 and also in 1998.

In this paper we describe in detail the photometric properties of the V4633 Sgr during the 1998–2000 seasons. We also report on a few spectroscopic observations that we performed on this star, and on the implications of these data on some properties of this system.

2 OBSERVATIONS AND DATA REDUCTION

2.1 Photometry

We performed photometry of V4633 Sgr during 34 nights in 1998, 36 nights in 1999, and 26 nights in 2000, using the Tektronix 1K back-illuminated CCD, mounted on the 1-m telescope at the Wise Observatory (WO). Details on the telescope and instrument are given by Kaspi et al. (1995).

Photometry was conducted either through an I filter, or switching sequentially between I and V, or between I, V and B filters. Logs of the observations are given in Appendix A.

★E-mail: yiftah@wise.tau.ac.il (YL); elia@wise.tau.ac.il (EML); ar@astro.keele.ac.uk and/or retter@physics.usyd.edu.au (AR); ohad@wise.tau.ac.il (OS)

Photometric measurements on the bias-subtracted and flat-field-corrected images were performed using the NOAO IRAF¹ DAOPHOT package (Stetson 1987). Instrumental magnitudes of V4633 Sgr, as well as of a few dozen reference stars, depending on image quality, were obtained for each frame. A set of internally consistent nova magnitudes was obtained using the WO reduction program DAOSTAT (Netzer et al. 1996). Good seeing conditions on 1998 September 19 were used to calibrate the magnitudes of V4633 Sgr, as well as of about a dozen nearby comparison stars. We used the calibrated comparison stars to convert all the measurements of V4633 Sgr into calibrated magnitudes.

In our programme we obtained 84 nights of continuous time series, accumulating a total of 8250 data points in I, 2392 in V and 756 in B.

On 2000 August 4, 20 and 21, we observed V4633 Sgr in the ‘fast photometry’ mode (Leibowitz, Ibbetson & Ofek 1999). On the first night we observed for 2.5 h, with time resolution of 10 s, using no filter (‘clear’). On the other two nights, we observed through an I filter, with time resolution of 20 s. The data were reduced in the manner described above.

2.2 Spectroscopy

V4633 Sgr was observed spectroscopically at WO on four nights: 1998 July 5 and August 30, and 1999 May 2 and July 6. The spectra were taken with the WO Faint Object Spectrograph and Camera (FOSC) described in Brosch & Goldberg (1994), and operated at the f/7 Ritchey–Chrétien focus of the WO 1-m telescope. The Tektronix 1K CCD was used as the detector. We applied the method of long-slit spectroscopy whereby both V4633 Sgr and a bright comparison star were included in the slit (see for example Kaspi et al. 2000). The comparison star used was non-variable to within ~ 2 per cent. We used a 10-arcsec wide slit along with a 600 line mm^{-1} grism, yielding a dispersion of 4 Å pixel^{-1} (~ 8 Å resolution). On the first two nights the spectrograph was set to cover the spectral range $\sim 3600\text{--}7200\text{Å}$, while in the last two nights we covered the range $\sim 4000\text{--}7800\text{Å}$. Two exposures of the spectrum of the nova were taken on each night.

Reduction of the bias-subtracted and flat-field-corrected spectra was carried out in the usual manner using IRAF with its SPECRED and ONEDSPEC packages. The spectra were dispersion-corrected using a He–Ar arc spectrum, which was taken on each night in between the pair of nova spectra. Each spectrum of the nova was divided by the spectrum of the comparison star observed simultaneously through the same slit. The two sets of nova/star spectrum ratios obtained on each night were compared to each other and were found to differ by no more than ~ 10 per cent. The average of the two ratios was then taken as the representative ratio for that night. The spectra were calibrated to an absolute flux scale by multiplying each mean nova/star ratio by a flux-calibrated spectrum of the comparison star. This spectrum, in turn, was flux-calibrated using the WO standard sensitivity function and extinction curve. These do not change appreciably from night to night, and they are updated from time to time at WO using spectrophotometric standard stars. The absolute flux calibration has an uncertainty of ~ 10 per cent, but the relative flux uncertainties within each spectrum are of order 2–3 per cent.

¹IRAF (Image Reduction and Analysis Facility) is distributed by the National Optical Astronomy Observatories, which are operated by AURA, Inc., under cooperative agreement with the National Science Foundation.

3 DATA ANALYSIS

Light curves of V4633 Sgr from discovery to 2000 July are presented in Fig. 1. The visual LC was compiled using data taken from VSNET.² The I, V and B LCs were compiled using data obtained in our programme. Note that the apparent small vertical lines in the I LC are not error bars but dense individual successive points observed in a single night. Bars representing the observational errors in our measurements are below the resolution limit of this figure.

The visual and V LCs show an apparent change in slope, becoming more moderate about three months after maximum light (Fig. 1). Most of the 1998 photometry was conducted around the time the slope changed. Shortly after, in 1998 July–August, the brightness of the star deviated systematically from the long-term trend given by the fitted curve, forming an apparent bump in the LC (Fig. 1, inset).

A panel of sample I-band LCs from different epochs is shown in Fig. 2. Nightly LCs show almost no visible variation until 1998 May. Fragmented LCs in May show some variation, while in June modulations on a time-scale of ~ 3 h are clearly visible. In July and August, the variations took other forms. In a few nights the variations are quasi-periodic but on a somewhat different time-scale than in June. On a few other nights, the brightness of the star varied monotonically during the entire nightly run. In all our subsequent observations in 1999 and 2000, the variations returned to the oscillation mode of 1998 June, albeit with an ever-increasing amplitude.

3.1 The 1999 light curve

We first discuss the data of 1999 since this season is better sampled than the other two. Fig. 3(C) shows the normalized power spectrum (PS) (Scargle 1982) of our 1999 I-band data, after eliminating the long-term decline by subtracting a fourth-degree polynomial from the 1998–1999 LC.

The PS is dominated by two similar alias patterns around two central frequencies, 7.7660 d^{-1} and 7.9628 d^{-1} , corresponding to the periodicities $0.128760 \pm 0.000013\text{ d}$ (hereafter P_1) and $0.125589 \pm 0.000016\text{ d}$ (P_2).

To derive the quoted periods, we performed a grid search in the χ^2 space, fitting to the data a polynomial term representing the secular decline of the nova and a pair of periods near the values of P_1 and P_2 obtained from the PS. The grid was then examined to find the pair of periods yielding the lowest value in the χ^2 space.

The errors of the two periods correspond to a 1σ confidence level, and were derived by a sample of 2000 bootstrap simulations (Efron & Tibshirani 1993).

We used the tests described in Retter, Leibowitz & Kovo-Kariti (1998) to confirm the independence of the two periodicities. Similar results were also obtained from the PSs of our 1999 V and B data sets.

At the right-hand side of Fig. 3(C), the first overtone of P_2 is detected at 15.928 d^{-1} , well above the noise level in its vicinity. Such a feature is expected, as a result of the asymmetric shape of the signal (see Section 3.6).

The lower end of the 1999 PS (Fig. 3C) is dominated by a structure of interdependent peaks, the highest of which, designated P_3 , is at 0.1976 d^{-1} (5.06 d) with a full amplitude of 0.096 mag. This periodicity corresponds to the beat period between P_1 and P_2 .

²VSNET = Variable Stars Network, Kyoto, Japan (<http://www.kusastro.kyoto-u.ac.jp/vsnet/>).

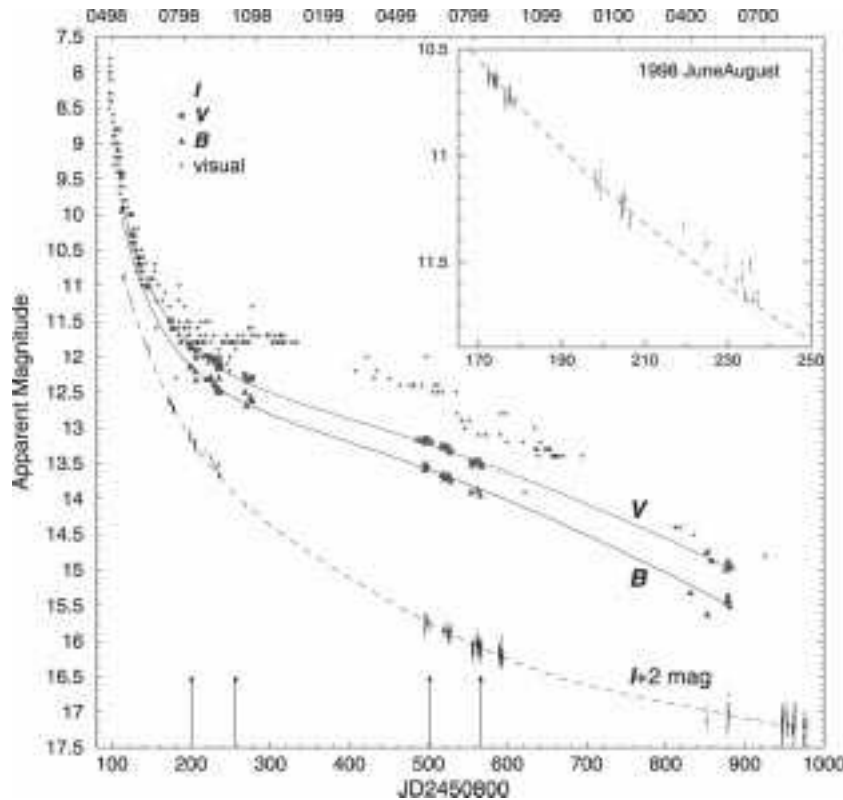


Figure 1. Light curves of V4633 Sgr. The points in the B and V LCs are mean magnitudes of each night of observations. The I LC comprises all the data points compiled in our observations. For convenience, the I LC was shifted down by 2 mag. The overlaid curves represent the long-term decline of the nova in each photometric band. The arrows at the bottom of the figure indicate dates of spectroscopic observations. The scale on the top axis is the date, in MM-YY format. The inset is a zoom-in view of the I LC during 1998 June–August, showing the ‘bump’ in the LC in August.

The signal was found to be independent of P_1 and P_2 . It was not detected in our V and B LCs. However, these data sets are of lower quality than the I data set, and span a shorter time. Owing to relatively high noise of the PS near P_3 and the fragmented nature of the LC on time-scales of a few days, the reliability of P_3 should be addressed with some caution, until it is confirmed by further observations.

In the 1999 I-band PS, the 1-d alias of P_2 , at 6.961 d^{-1} , is stronger than the peak associated with P_2 (Fig. 3C). The same result occurred in a few other tests we conducted, for various subsets of the data, as well as in the different bands and data sets, and using various detrending methods. Similarly, in a small number of tests the signal at 6.76 d^{-1} , or the one at 8.76 d^{-1} , dominated the alias structure of P_1 , rather than the one at 7.76 d^{-1} .

These results introduce some uncertainty into our selection of 7.76 d^{-1} and 7.96 d^{-1} for P_1 and P_2 , respectively. However, we consider this selection firm, because of the dominance of these periods in the bulk of our tests. Further support to this selection comes from the presence in the PS of the first overtone of 7.96 d^{-1} , and the absence of any noticeable signal at the frequency of the expected first overtone of 6.96 d^{-1} (Fig. 3C, inset). The presence in the PS of P_3 – the beat of 7.76 d^{-1} and 7.96 d^{-1} – is yet another strong argument for selecting these two periods.

3.2 The 1998 May–June light curve

The PS of the I-band data obtained during six nights in 1998 June (Fig. 3A) resembles that of 1999. Two peaks at 7.782 and 7.999 d^{-1} , each of which is the centre of a 1-d, $\frac{1}{2}$ -d, $\frac{1}{3}$ -d (etc.) alias

pattern, dominate the PS. The group of peaks at the lower end of the PS are of questionable reliability owing to the short time-span of the data set, and since they are sensitive to the method used to detrend the strongly declining LC.

The values of P_1 and P_2 , derived by simultaneously fitting two periods and a linear term to the LC, are $0.12893 \pm 0.00015 \text{ d}$ and $0.12523 \pm 0.00033 \text{ d}$. A peak at 15.52 d^{-1} (Fig. 3A) probably corresponds to the first overtone of P_1 , which is expected at this frequency.

Adding the fragmentary time series obtained in 1998 May to the June data, the power of the two peaks corresponding to P_1 and P_2 increased in the combined PS (not shown), relative to the PS of June only. Indeed, examination of the short LC of May revealed a hump that is in fair agreement with the modulations of the June LC, extrapolated to the times of observation in May. Thus, it is likely that the light of the star was modulated by at least one of the two periodicities as early as 1998 May.

3.3 The 1998 July–August light curve

The PS of the V-band data gathered during 13 nights in 1998 July–August (Fig. 3B) is different in its structure and details from the former two PSs. A broad excess of power in the vicinity of 5 d^{-1} dominates the PS, but no obviously significant peak stands out above the wide hump. Looking for the known periodicities, a peak at 7.756 d^{-1} is found (marked with an arrow in Fig. 3B). However, this peak is well within the noise level and there is a high a priori probability for its presence in the PS as a result of random coincidence. The July–August data are therefore consistent with

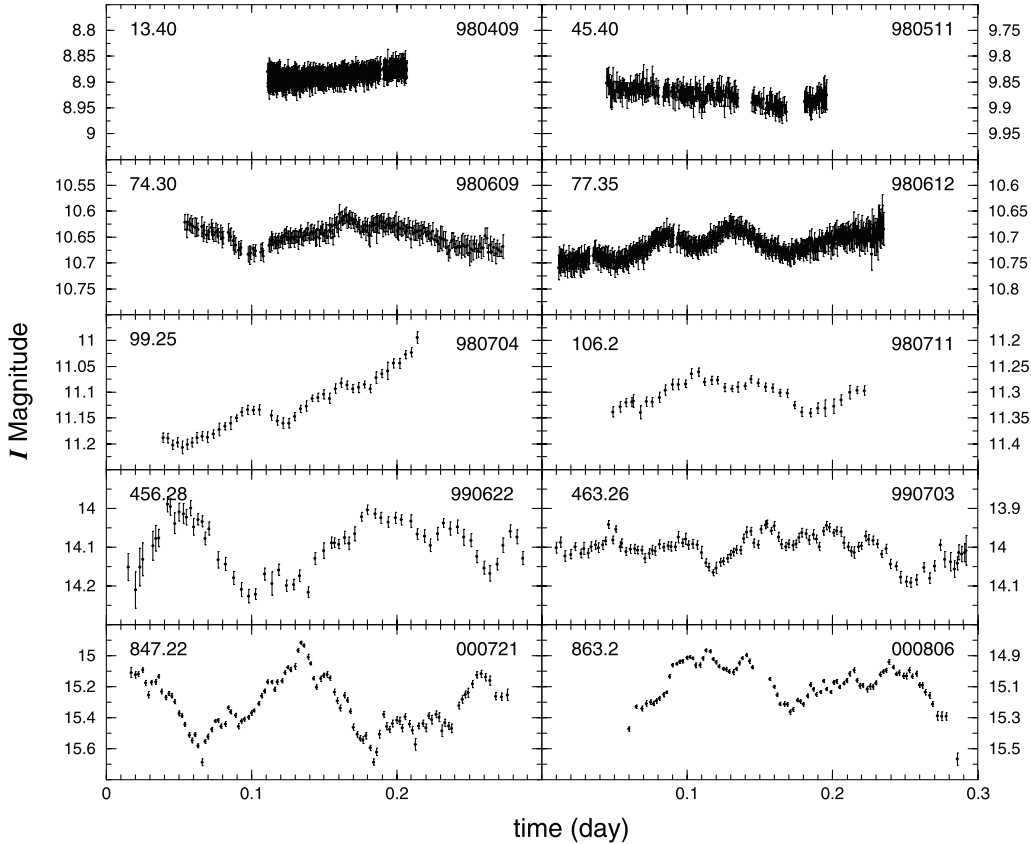


Figure 2. A sample of nightly light curves of V4633 Sgr from different epochs. On the left of each frame is the time (HJD $-245\,0900$) of the beginning of observation. The date of observation is on the right of each frame, in YYMMDD format. Note the difference in the y-axis scales.

an LC that is not significantly modulated by either of the periods P_1 or P_2 .

To test further the difference between the July–August data and that of June, we constructed an artificial LC by extrapolating the signals of the June LC on to the actual times of observation of the July–August LC. Comparing the observed LC and the artificial one, there was only little resemblance between the two in the phases and shapes of the modulations. Also, in contrast to the PS of the actual data (Fig. 3B), the periods of 1998 June were clearly detectable in the PS of the artificial LC.

3.4 The 2000 light curve

The PS of the I-band data of 2000 (Fig. 3D) is dominated by the signal of P_1 at 7.795 d^{-1} . The signal of P_2 , at 7.964 d^{-1} , is obscured by the alias structure of P_1 , but becomes the dominant feature in the residual PS once P_1 is removed from the data. A weak signal at 15.929 d^{-1} is probably the first overtone of P_2 . A simultaneous fit of two periods and a linear term to the data yields the best-fitting values $P_1 = 0.128292 \pm 0.000007\text{ d}$ and $P_2 = 0.125570 \pm 0.000010\text{ d}$.

Finally, we looked for periodic variations in the data accumulated in the three 2000 nights of fast photometry (Section 2.1). We found no sign in the data for any periodicity in the range of a few tens of seconds to a few tens of minutes.

3.5 Stability of the signals

The value of P_2 measured in 2000 is just 0.015 per cent smaller

than in 1999. The difference amounts to only 1.2σ of the uncertainty in the derived value of the periods themselves. The two values are therefore consistent with the notion that P_2 is the same in both years. This is not the case for P_1 . The value measured in 2000 is 0.3 per cent smaller than in 1999, and the difference is highly significant, more than 30σ .

To examine further the stability of the periodicities, we measured P_1 and P_2 in six different data sets during the 1998–2000 time interval, in the manner described in Section 3.1. The measured values of P_2 are scattered around the average value of 0.12559 d , although a linear fit yields a formal rate of period change $\dot{P}_2 = (-1.7 \pm 0.7) \times 10^{-7}$ (Fig. 4, bottom panel). We consider this result as consistent with a constant period. The slope for P_1 is highly significant: $\dot{P}_1 = (-1.26 \pm 0.05) \times 10^{-6}$ (Fig. 4, top panel).

3.6 Waveforms and amplitudes

The waveforms of P_1 and P_2 in 1998 June, 1999 and 2000 are shown in Fig. 5. In each case, we ‘pre-whitened’ the LC before folding by removing the signal of the other periodicity, as well as a polynomial term representing the decline in the brightness of the nova. In the 1999 data set P_3 was subtracted as well.

The waveform of P_1 was symmetric during the three observational seasons. In 1998 June, a clear dip of 0.012 mag was imposed on the primary maximum. In 1999 the waveform transformed into a nearly sinusoidal shape, which was maintained also in 2000 (Fig. 5, left panels). The peak-to-peak amplitude of P_1 was 0.030 mag in 1998 June, 0.105 mag in 1999 and 0.25 mag in 2000.

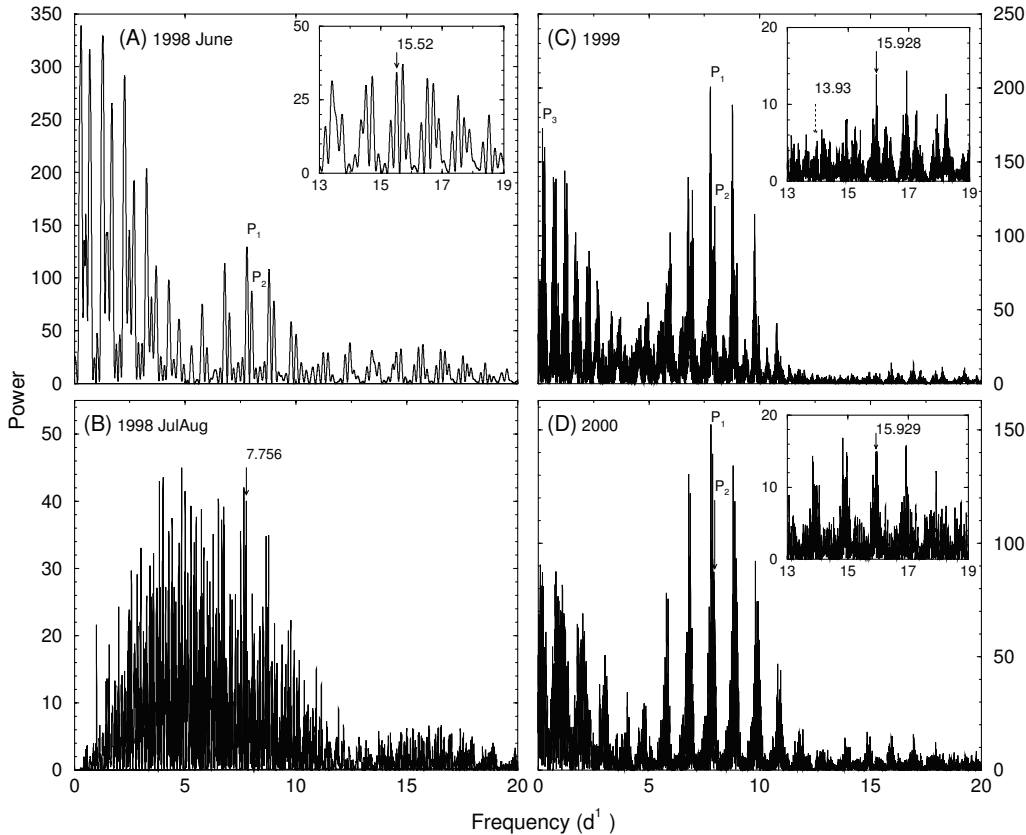


Figure 3. Normalized power spectrum of four data sets. The peaks corresponding to P_1 and P_2 are marked in each PS. (A) The 1998 June I data set. The peak marked in the inset frame probably corresponds to the first overtone of P_1 . (B) The 1998 July–August V data set. A night of monotonic trend was excluded. The data were pre-whitened by subtracting the mean magnitude from each night. An arrow marks a peak at 7.756 d^{-1} , which is the seventh highest peak in the PS. (C) The 1999 I data set. The low end of the PS is dominated by P_3 , at 0.1976 d^{-1} . The first overtone of P_2 , at 15.928 d^{-1} , is marked in the inset. The first overtone of the 6.963 d^{-1} 1-d alias of P_2 is expected at 13.926 d^{-1} (marked by a dashed arrow in the inset). However, no noticeable signal is detected in the vicinity of this frequency. (D) The 2000 I data set. The first overtone of P_2 is marked in the inset.

P_2 maintained an asymmetric shape during the three observational seasons, with a slow rise and a fast decline (Fig. 5, right panels). The peak-to-peak amplitude of P_2 was 0.019 mag in 1998 June, 0.100 mag in 1999 and 0.19 mag in 2000.

The waveforms of P_1 and P_2 in 1999 in V and B, as well as those obtained from the much limited V-band data in 1998 June and in 2000, were similar to the ones in I.

The limited data in V and B do not allow an accurate tracking of the amplitudes of the two signals. However, some information on the change in amplitude may be gained by inspecting the secular change in nightly variation, e.g. by following the secular change in the standard deviation (STD) of nightly LCs. The variation in I steadily increased by about 0.05 mag yr^{-1} during 1998–2000, consistent with the increasing amplitudes of the two periodicities described above. The STD of the V magnitudes has not changed significantly in 1998–1999, maintaining a value of $\sim 0.027 \text{ mag}$, and increased in 2000 to $\sim 0.073 \text{ mag}$. In B it decreased, from $\sim 0.040 \text{ mag}$ in 1998 to $\sim 0.023 \text{ mag}$ in 1999. One should bear in mind that these trends reflect not only changes due to the brightness variations of sources within the binary system of V4633 Sgr but also some varying contribution of the nebula to the total light of the source. Thus, during 1998–1999 the contribution of the nebula in the V band increased from 40 per cent to about 70 per cent (Section 3.7), implying that the amplitude of the variations in the stellar V continuum was in fact larger than indicated by the STD values.

3.7 Spectroscopy

Four spectra obtained at WO in 1998–1999 are plotted in Fig. 6. Fluxes of a few of the emission lines are shown in Table 1. The spectrum of 1998 July 5 features prominent Balmer lines as well as the strong auroral line $[\text{N II}] \lambda 5755$. The nebular lines $[\text{O III}] \lambda \lambda 4959, 5007$ are also seen. By 1998 August 30, $[\text{O III}] \lambda \lambda 4959, 5007$ and $[\text{O III}] \lambda 4363$ became stronger, and the Balmer lines and $[\text{N II}] \lambda 5755$ faded. The two spectra of 1999 were dominated by the $[\text{O III}] \lambda \lambda 4959, 5007$ lines. The decline of the Balmer lines and $[\text{N II}] \lambda 5755$ continued, while the auroral line $[\text{O III}] \lambda 4363$ became more dominant. Higher ionization lines of $[\text{Fe VII}]$ appeared and became stronger. All four spectra are in the auroral phase, according to the Tololo classification system (Williams et al. 1991; Williams, Phillips & Hamuy 1994). The 1998 July 5 spectrum is probably classified A_n , and the other three spectra are probably in the A_o phase.

In each of the spectra we calculated the integrated V magnitude of the star by convolving the observed spectral energy distribution with the transmission curve of the V filter. The results agreed with the values obtained from photometry. The spectra also allowed us to subtract from the integrated V brightness the contribution of the emission lines that originate mostly in the nebula. As expected, when considered alone, the V continuum faded faster than the integrated V magnitude, with $V_{\text{continuum}} - V_{\text{total}} = 0.55, 0.92, 1.28$ and 1.26 mag on 1998 July 5, 1998 August 30, 1999 May 5 and 1999 July 6, respectively.

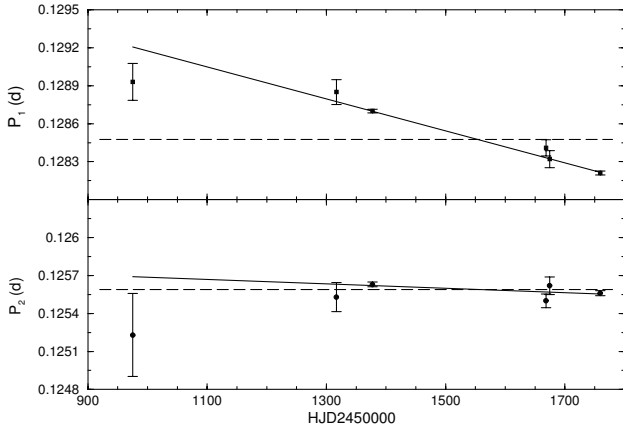


Figure 4. Variation of P_1 (top panel) and P_2 (bottom panel) in 1998–2000. Solid lines are linear fits to the data. Dashed lines are the weighted average of the measured periods.

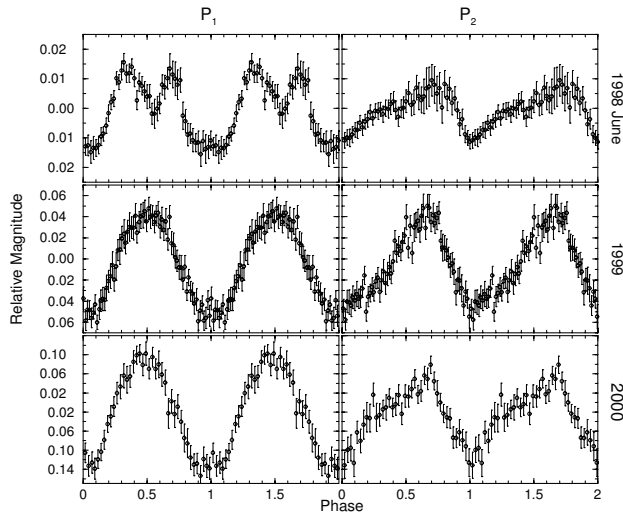


Figure 5. The ILCs of the three observational seasons folded on the period of P_1 (left), and on P_2 (right). Discrete points are mean magnitudes in each of 50 equal bins covering the 0–1 phase interval. The inserted bars are the standard deviation in the value of the mean in each bin. Note the difference in the y-axis scales.

4 DISCUSSION

4.1 The two periods in the LC of V4633 Sgr

The photometric data of the three-year observations of V4633 Sgr confirm the presence of two independent periodicities in the LC of V4633 Sgr: $P_1 = 3.08 \text{ h} = 0.1285 \text{ d}$ and $P_2 = 3.014 \text{ h} = 0.125576 \pm 0.000009 \text{ d}$.

We suggest that P_2 is the orbital period of the underlying binary system, as its behaviour during the three years of photometry is consistent with a stable period. In addition, during the photometric monitoring, the waveform of the signal has maintained its shape. The asymmetric shape of the waveform is rather unique for orbital modulations; none the less, we note its close similarity to the shape of the orbital modulation of V1974 Cyg in 1996 (Skillman et al. 1997). The 3.01-h period is well situated within the range of orbital periods of cataclysmic variables. To confirm this suggestion, radial

velocity measurements should be carried out. In the following we shall consider P_2 to be the orbital period, P_{orb} , of the binary system.

4.2 The second periodicity

It is more difficult to interpret the longer period, P_1 . This signal is characterized by the following traits: (1) it is ~ 2.5 per cent longer than the binary period; and (2) it is at least an order of magnitude less stable than P_{orb} , decreasing by ~ 0.3 per cent during 1999–2000, with $\dot{P} \sim -10^{-6}$ (Section 3.5).

Two possible interpretations come to mind. One is that the origin of the P_1 variation is the rotation of the white dwarf (WD). The modulation may arise, for instance, from aspect variation of a hotspot on or near the surface of the WD. The small deviation of P_1 from the orbital period would then suggest that V4633 Sgr belongs to the asynchronous polars group (BY Cam stars, hereafter APs). An alternative interpretation is that the origin of P_1 is in an accretion disc in the system, namely, that it is the period of the well-known phenomenon of superhumps (SHs).

In the following two sections we discuss the two interpretations and some of their implications. The data to hand seem insufficient to make a reliable choice between them.

4.3 Asynchronous polar interpretation

APs are a subclass of magnetic cataclysmic variables, sharing many of the properties of polars (AM Her stars), but having a WD that rotates with a period that differs by ~ 1 per cent from the orbital period. There are four known APs. They are listed in Table 2 along with the major characteristics of their periodicities. In one AP, V1500 Cyg, the asynchronous rotation is clearly associated with its nova eruption in 1975. Two other APs are suggested to have also undergone a recent nova event: V1432 Aql (Schmidt & Stockman 2001) and BY Cam (Bonnet-Bidaud & Mouchet 1987).

The AP interpretation of V4633 Sgr is supported by the monotonic decrease in P_1 , the proposed rotation period of the WD (P_{rot}), towards synchronization with P_{orb} . A synchronization trend in P_{rot} is expected in APs as a result of the magnetic torque exerted on the WD by the secondary star. Indeed, such a trend was detected in three of the four APs (Table 2). Also, the orbital period of V4633 Sgr, $P_{\text{orb}} = 3.01 \text{ h}$, is similar to that of three APs (Table 2). The beat period, $P_3 = 5.06 \text{ d}$, detected in 1999 (Section 3.1), may be naturally explained in the AP framework. If a dipole geometry is assumed, pole switching is expected to occur at the beat cycle, modulating the LC at P_{beat} .

However, a simple AP interpretation seems to be inapplicable in V4633 Sgr for the following reasons:

(i) The synchronization rate of the proposed P_{rot} is $|\dot{P}_1| \sim 10^{-6}$ – much larger than in APs, where $|\dot{P}_{\text{rot}}| \sim 3 \times 10^{-9}$ to 4×10^{-8} (Table 2).

(ii) In V4633 Sgr, P_1 is longer than P_{orb} , while in three of the four APs P_{rot} is shorter. In V1432 Aql, the only AP in which $P_{\text{rot}} > P_{\text{orb}}$, the difference is marginal. Even so, the longer P_{rot} poses some theoretical difficulties [we note, however, that Schmidt & Stockman (2001) argue that $P_{\text{rot}} < P_{\text{orb}}$ is a possible outcome of a nova eruption, in slow novae with strong magnetic fields]. Indeed, an alternative model for this object was proposed by Mukai (1998), in which V1432 Aql is an intermediate polar with a spin period of 1.12 h.

(iii) The difference between the two periods in V4633 Sgr is

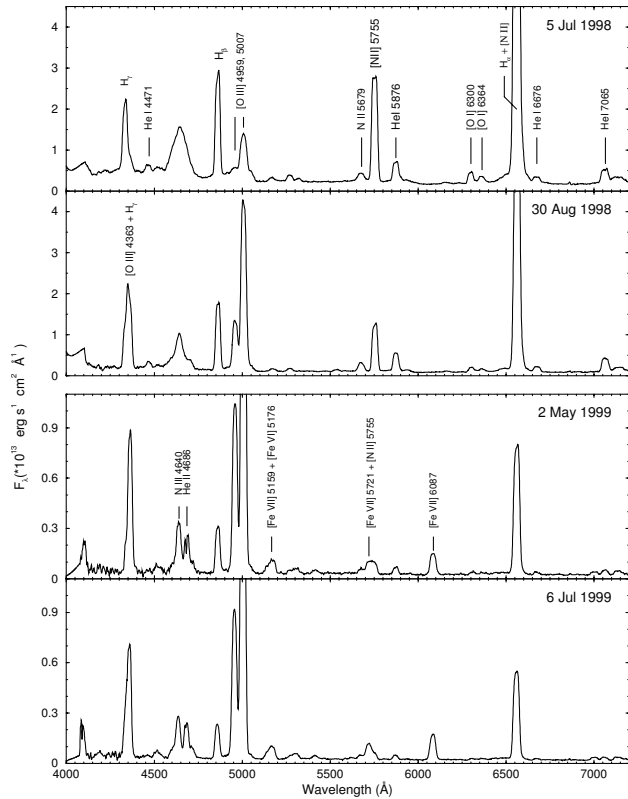


Figure 6. Spectra of V4633 Sgr obtained at WO. Each emission-line identification is given only on the initial appearance of that line in the spectrum, and it remains valid for later spectra.

Table 1. V4633 Sgr. Intensity of selected emission lines relative to $H\beta$. The estimated uncertainties range from 3 per cent in the strongest lines, to about 10 per cent in weak lines.

Line identification	Flux ($H\beta = 100$)			
	980705	980830	990502	990706
$H\gamma$ /[O III] 4363	86	163	344	424
He I 4471	7.3	8.4		
$H\beta$	100	100	100	100
[O III] 4959	4.9	73	407	491
[O III] 5007	58	300	1246	1492
N II 5679	13.0	15.4		
[N II] 5755	141	83		
He I 5876	23	31	18.2	14.9
[Fe VII] 6085			64	98
[O I] 6300	13.1	9.1		
[O I] 6364	8.8	6.5		
$H\alpha$ + [N II]	678	520	381	352
He I 6676	5.5	9.1	7.2	5.6
He I 6065	16.2	27	12.6	13.9
$H\beta$ ($\times 10^{-13} \text{ erg s}^{-1} \text{ cm}^{-2}$)	77	50	7.9	5.7

~ 2.3 per cent – larger than the value in any of the four APs (Table 2).

(iv) The distinctly asymmetric waveform of P_{orb} in V4633 Sgr is hardly that of an eclipsing system (Section 3.6). If there is no disc in the system, as the AP model suggests, the light modulation on the orbital period must be ascribed to the ‘reflection’ effect. Any simple model of this effect produces symmetric binary LCs.

(v) If the modulation at P_{beat} is caused by pole switching, the latter is expected also to affect P_1 , invoking a phase shift of 180° twice every beat cycle. This effect should reveal itself both in the PS, reducing the power of the peak associated with P_1 , and in the folded LC of P_1 . However, these effects are not detected.

Few of the distinctive characteristics of V4633 Sgr may be explained in the framework of the AP model if they are attributed to short-term changes taking place in the system in the first few years after the nova outburst. Such an irregular behaviour was observed in V1500 Cyg during the first three years after its outburst. These have been described in detail (e.g. Patterson 1979; Lance, McCall & Uomoto 1988) and interpreted by Stockman, Schmidt & Lamb (1988).

Applying the model of Stockman et al. (1988) to V4633 Sgr, we should assume that the spin of the WD was synchronized with the orbital revolution prior to the nova event. The rapid expansion of the WD’s envelope during the first stages of the outburst increased the star’s moment of inertia, resulting in a spin-down of the WD by ≥ 2.5 per cent. The decrease in P_{rot} in 1998–2000 should be attributed to the contraction of the still expanded envelope of the WD, with the associated reduction in its moment of inertia. Thus, P_{rot} is expected to continue decreasing until the WD finally regains its original radius. Following this, a slower synchronization trend is expected to occur on the magnetic synchronization time-scale of the system. In analogy with V1500 Cyg, if the contraction of the envelope decreases the moment of inertia of the WD by a magnitude comparable to that gained during the nova outburst (Patterson 1979; Stockman et al. 1988), and if the spin acceleration rate maintains its value of 1999–2000 (Section 3.5), the WD would regain its pre-nova dimension around the year 2006.

For an order-of-magnitude calculation, we attribute the change in P_1 in 1998 June–2000 entirely to the contraction of the WD’s envelope. We further assume that the WD is a rigid sphere of mass M_1 and radius R_1 , rigidly coupled to a thin shell of mass M_{ph} and radius R_{ph} . Let ΔR_{ph} and $\Delta\omega$ be the changes in the radius and the angular velocity of the WD during a time interval Δt . Conservation of angular momentum requires that

$$\frac{2}{3}M_{\text{ph}}[(R_{\text{ph}} + \Delta R_{\text{ph}})^2 - R_{\text{ph}}^2] \approx -\frac{2}{5}M_1 R_1^2 \frac{\Delta\omega}{\omega + \Delta\omega}.$$

Since in 2000 August, $R_{\text{ph}} \geq R_1$, the photosphere radius at time Δt prior to 2000 August is bounded by

$$R_{\text{ph}} \geq \sqrt{\frac{3M_1}{5M_{\text{ph}}} \frac{\Delta\omega}{\omega + \Delta\omega}} R_1.$$

From the speed class of V4633 Sgr ($t_3 \approx 42$ d, Section 4.5.1) we infer $M_1 \approx 1.1 M_\odot$ for the mass of the WD (Kato & Hachisu 1994). As a rough estimate of the mass of the contracting envelope we take $M_{\text{ph}} \sim 10^{-6} M_\odot$ (Priyalnik 1986; Priyalnik & Kovetz 1995). Inserting these values into the above equation together with the observed values of P_1 , we obtain $R_{\text{ph}} \geq 71R_1$ and $53R_1$ in 1998 June and 1999 May, respectively.

The scenario depicted above is considerably different from the

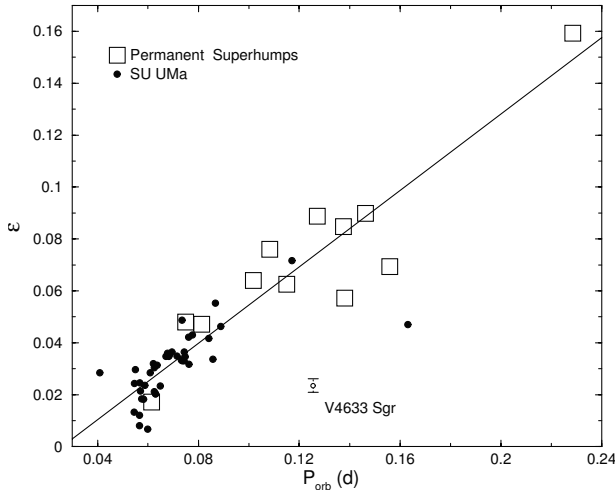


Figure 7. The period excess– P_{orb} relation of superhump systems. Data were taken from Patterson (1998, 1999) and Retter et al. (2001). The solid line is a linear fit to the data.

one in V1500 Cyg. In particular, in the 1975 nova outburst, the WD and its envelope gained angular momentum through coupling with the orbiting secondary during the common envelope phase, almost resynchronizing the WD’s spin with the orbital cycle within a few tens of days after outburst. This is why, in that system, P_{rot} became shorter than P_{orb} as the WD’s envelope contracted. In V4633 Sgr such a coupling either did not take place at all, or was much less effective in transferring orbital to spin angular momentum. It is therefore also likely that this system will remain with a spin period longer than the binary period even after the WD regains its pre-outburst dimension.

Some other different aspects in the evolution of V4633 Sgr, such as the apparently larger increase in P_{rot} during the outburst, and the longer time-scale of the envelope contraction, may be attributed to a less massive WD, which is expected to shed more mass during outburst, and regain its original size on a longer time-scale (Kato & Hachisu 1994; Prialnik & Kovetz 1995).

The AP interpretation should be tested against an observational search for evidence for the magnetic nature of V4633 Sgr. This should manifest itself, for example, by strong X-ray radiation and/or circularly polarized light, modulated by the WD rotation period. So far no such observations (or results) have been reported.³

4.4 Permanent superhump interpretation

Superhumps (SHs) are periodic brightness variations in the LCs of certain subgroups of disc-accreting cataclysmic variables (CVs), with a period a few per cent longer than the orbital period of the binary system (Warner 1995).

Initially, SHs were found in the SU UMa subclass of dwarf novae during superoutburst events. SHs of longer duration, of months and years, are termed ‘permanent SHs’. They appear in LCs of CVs with short orbital periods (typically $P_{\text{orb}} \lesssim 4$ h; Patterson 1999) and high mass transfer rates, such as nova remnants, nova-like and AM CVn systems (for reviews see

³Non-detection of linear polarization in 1998 March (Ikeda et al. 2000) is of small relevance, since, at that early epoch in the history of the outburst, any polarization would be masked by the luminous extended photosphere and ejecta. Naturally, as the nova continues to fade, detection of circular polarization becomes increasingly feasible.

Table 2. Periods of asynchronous polars. The values for V4633 Sgr are given at the bottom for reference.

	P_{orb} (h)	P_{rot} (h)	$\frac{P_{\text{orb}} - P_{\text{rot}}}{P_{\text{orb}}}$ (per cent)	\dot{P}_{rot}
V1500 Cyg ^{a,b}	3.35	3.29	1.7	4×10^{-8}
BY Cam ^c	3.35	3.32	0.9	4×10^{-9}
V1432 Aql ^{d,e}	3.36	3.37	−0.3	-1×10^{-8}
CD Ind ^f	1.85	1.83	1.1	
V4633 Sgr ^g	3.01	3.08	−2.3	-1.26×10^{-6}

^aSchmidt, Liebert & Stockman (1995); ^bKaluzny & Semeniuk (1987); ^cMason et al. (1998); ^dPatterson et al. (1995); ^eGeckeler & Staubert (1997); ^fRamsay et al. (1999); ^gthis work.

Patterson 1999; Retter & Naylor 2000). Superhumps also occur in X-ray binaries (e.g. O’Donoghue & Charles 1996).

The properties of V4633 Sgr make it a good candidate for hosting the SH phenomenon. The 3.01-h orbital period puts V4633 Sgr near the centre of the period interval that contains most of the known SH systems (Patterson 1998).

The observed stable decline in the brightness of the nova is consistent with the presence in the system of an accretion disc, which in the years 1999–2000 is the main source of the optical luminosity, and which is thermally stable. If mass accretion is indeed the main luminosity source, we can estimate its rate using equation (3) of Retter & Naylor (2000). In terms of absolute magnitude it is given by

$$\dot{M}_{17} = [10^{(M_V - 5.69 + \Delta M_i)/(-2.5)}] \frac{1}{M_1^{4/3}},$$

where \dot{M}_{17} is the mass transfer rate in 10^{17} g s^{-1} , M_V is the absolute V magnitude of the disc, M_1 is the mass of the WD, and $\Delta M_i = -2.5 \log[(1 + 1.5 \cos i) \cos i]$ is a correction to the magnitude due to the inclination angle (i) of the disc. From the V-band LC (Fig. 1), and the estimated distance and reddening towards V4633 Sgr (Section 4.5.4), we derive $M_{V,2000} \sim 0.5$ –1.5. The non-eclipse shape of the LC (Section 3.6) implies that the inclination angle is $i \leq 65^\circ$. For a $M_1 \approx 1.1 M_\odot$ WD, we obtain $\dot{M} \sim (30$ – $300) \times 10^{17} \text{ g s}^{-1}$. The critical mass transfer rate, below which the disc is thermally unstable, is given by Osaki (1996, equation 4 therein), which for $P_{\text{orb}} = 3.01$ h takes the value $\dot{M}_{\text{crit}} \approx 1.7 \times 10^{17} \text{ g s}^{-1}$. Thus the observed mass transfer rate in V4633 Sgr is some two orders of magnitude above the critical value, and the disc is indeed thermally stable.

Superhumps are known to be poor clocks. In permanent SH systems, the instability in superhump period is: $\dot{P}_{\text{SH}} = 10^{-8}$ to 5×10^{-6} (Patterson & Skillman 1994). The value of \dot{P}_1 that we found in V4633 Sgr in 1999–2000 is within this range.

The similarity in the shape of the orbital and the superhump waveforms of V1974 Cyg to those of P_2 and P_1 (Skillman et al. 1997) serves as a further support to the SH interpretation.

On the weak side of the SH interpretation stands the value of the period excess $\epsilon \equiv (P_{\text{SH}} - P_{\text{orb}})/P_{\text{orb}}$. Superhump systems are known to follow a nearly linear relation between ϵ and P_{orb} (Stolz & Schoembs 1984). In V4633 Sgr the measured value, $\epsilon = 0.024 \pm 0.003$, is about a third of the value expected for $P_{\text{orb}} = 3.01$ h (Fig. 7). Inspection of Fig. 7 reveals, however, that, while the point of V4633 Sgr deviates the most from the empirical linear

relation, it is not qualitatively exceptional. All other points representing permanent SH systems (open squares) are distributed with a rather large scatter around the regression line. Two of them, V603 Aql and BH Lyn, show an exceptionally large deviation relative to the other systems. We should also note that the apparent large deviation of the black dot representing the SU UMa system CN Ori should be treated with caution, until its period excess is confirmed by further observations (Patterson, private communication).

Since the disc precession is caused by the perturbation of the secondary star, the precession rate should be proportional to the secondary's mass, M_2 . Such a relation was found by Osaki (1985), who examined the motion of a free particle in a binary potential. In particular, for a disc with radius ≈ 0.46 times the binary separation (this is approximately the disc radius at the 3:1 resonance where SH are most likely to occur), Osaki derived the relation

$$\frac{P_{\text{orb}}}{P_{\text{beat}}} \approx 0.233 \frac{q}{\sqrt{1+q}},$$

where $q \equiv M_2/M_1$. For V4633 Sgr, this relation yields the value $q \approx 0.10$ – 0.11 . Since the mass of the WD should be smaller than the Chandrasekhar mass ($1.44 M_{\odot}$), the mass of the secondary is bounded by $M_2 \lesssim 0.16 M_{\odot}$.

On the other hand, if the secondary is a Roche lobe filling, main-sequence star, its mass can be derived analytically (e.g. Warner 1995), if P_{orb} is known. An empirical $P_{\text{orb}}-M_2$ relation yields a result similar to the analytical ones (Smith & Dhillon 1998). For $P_{\text{orb}} = 3.01$ h, the mass of a main-sequence secondary is $M_2 \approx 0.27 M_{\odot}$, much larger than the limit obtained above.

This inconsistency may infer that the cause of the exceptionally small ϵ may be an undermassed secondary star, which is off the main sequence. In this case, V4633 Sgr may be an extremely evolved CV system (e.g. Howell, Rappaport & Politano 1997; Patterson 1998).

The 5.06-d signal observed in 1999 (P_3 , Section 3.1) presents another difficulty for the permanent SH scenario. This period corresponds to the beat period between P_{orb} and P_{SH} . It is therefore natural to interpret this signal as arising from the precession of the accretion disc. However, theoretically, apsidal precession of an eccentric disc is not expected to modulate the light of the nova (Skillman & Patterson 1993; Patterson 1998). We note however that such modulations were actually observed in the permanent SH system AH Men (H0551-819) in 1993–94, when the object showed positive SH (Patterson 1995).

The permanent SH interpretation may be tested photometrically during the next few years. Superhump periods are found to wander about a mean value, and therefore \dot{P}_{SH} is expected occasionally to change its sign.

4.5 Further parameters of V4633 Sgr

4.5.1 The visual light curve

We derive some of the properties of the visual LC of V4633 Sgr using magnitudes of the nova published in the IAU Circulars and in the VSNET website, and the LC presented by Liller & Jones (1999).

The data suggest that the nova was discovered before reaching maximum brightness, as was already pointed out by Liller & Jones (1999). However, the scatter in magnitude estimates during the first few days after discovery does not allow us to determine the exact timing and magnitude of maximum brightness. We can only

conclude that the nova reached maximum light sometime between JD 245 0895.5 and 245 0898.5. We adopt the value of $m_{v,0} = 7.7 \pm 0.1$ for its visual magnitude at maximum.

From the VSNET data we estimate decline rates of $t_{2,v} = 19 \pm 3$ d and $t_{3,v} = 42 \pm 5$ d, somewhat longer than the estimation of Liller & Jones (1999) – $t_{3,v} \approx 35$ d.

By the classification scheme of Duerbeck (1981), V4633 Sgr should be classified as a Ba-type nova – moderately fast with minor irregular fluctuations during decline.

4.5.2 Photometric changes in 1998 June–August

Around 1998 June, there was an apparent bend in the visual and V LCs (Section 3, Fig. 1). Leibowitz (1993) noted that such a feature is found in the visual LCs of many classical novae, and suggested attributing it to the decay of the WD's light level below the brightness emitted by the accreted material. This interpretation was cast into quantitative form in models suggested recently by Hachisu et al. (2000) and Hachisu & Kato (2000) for the LCs of the two recurrent novae V394 CrA and U Sco.

Shortly after the change in the slope of the LC, in 1998 July–August, the I LC deviated from its smooth decline, forming an apparent bump. A similar bump was seen in the B and V LCs (Section 3, Fig. 1, inset). Two of our spectra, taken at the same time, on 1998 July 5 and August 30, show the emergence of strong [O III] $\lambda\lambda 4959, 5007$ emission lines (Section 3.7). The simultaneous occurrence of the two effects was observed in a few other novae, and was connected with the beginning of the nebular stage (Chochol et al. 1993).

During July–August another photometric peculiarity occurred – the LC was modulated in a different form than previously. In particular, the periodicities of 1998 June were not detected during these months (Section 3.3). We offer no explanation for this phenomenon, or to its possible connection to the aforementioned phenomena.

4.5.3 Interstellar reddening

We can estimate the interstellar reddening towards V4633 Sgr in three ways. First, we consider the observed Balmer decrement in the spectra of the nova. {In the following we neglect the contribution of the [N II] $\lambda\lambda 6548, 6584$ lines to the measured $H\alpha$ line intensity. From the [O III] (5007 + 4959)/4363 line ratio and the [N II] 5755 line intensity (Osterbrock 1989), we estimate it to be less than 5 per cent of the measured flux.} Slightly more than three months after maximum, the line intensity ratio $H\alpha/H\beta$ was as high as 6.8, probably due to self-absorption (Williams 1994). Our spectra show the progressive decrease of this line ratio during the following year. Between our last two spectroscopic observations the trend of decrease has flattened considerably. About 15 months after outburst, in our last spectrum measurement, this line ratio reached the value 3.52 ± 0.10 (Table 1). Attributing the difference between this value and the theoretical case B value of 2.8 (Osterbrock 1989) entirely to dust extinction, and using the numerical form of the Whitford (1958) reddening curve given by Miller & Mathews (1972), we obtain a reddening of $E(B - V) = 0.21 \pm 0.03$.

A second way to estimate the reddening is from the He triplet ratio, $5876/4471 = 2.9$, which seems to be insensitive to radiation transfer effects (Ferland 1977). The observed ratio on 1998 August 30 was 3.7 ± 0.4 , leading to $E(B - V) \sim 0.23$, in agreement with

the value derived from the H lines. We did not measure this line ratio in the spectrum of 1998 July 5, because the uncertainty in the measurement of the He $\lambda 4471$ line was much larger at that epoch. We note that, as pointed out by Ferland (1977), this method is inaccurate as a result of the small baseline and also the weakness of the He $\lambda 4471$ line.

We also estimated the reddening using colour photometry of the nova shortly after outburst. Novae have intrinsic colours $(B - V)_0 = +0.25 \pm 0.05$ at maximum (Downes & Duerbeck 2000) and $(B - V)_0 = -0.02 \pm 0.04$ at 2 mag below maximum light (van den Bergh & Younger 1987). Observations in the B and V bands by S. Kiyota, reported in VSNET, yield a colour index $(B - V) = +0.50$ on 1998 March 25, slightly below maximum light, and $(B - V) = +0.24$ on 1998 April 19, slightly below maximum plus 2 mag. At these two dates, the intrinsic colour of the nova was somewhat redder than the corresponding two ‘standard’ values quoted above. The difference between the two pairs of values constrains the interstellar reddening towards the nova to $E(B - V) \leq 0.25$, in agreement with the value derived from spectroscopy.

The small degree of reddening towards V4633 Sgr was noticed also by Rudy et al. (2000). The survey of Neckel & Klare (1980) confirms the relatively low extinction towards V4633 Sgr ($A_V \approx 0.65$, if we use $R = A_V/E(B - V) = 3.1$). The Galactic coordinates of V4633 Sgr are $(l, b) = (5.128, -6.231)$, and its estimated distance is $d \approx 9$ kpc (Section 4.5.4). The corresponding field in Neckel & Klare (1980) is 237, for which they found $A_V \approx 0.6-1.1$ at distances of 5–8 kpc.

4.5.4 Maximum magnitude and distance

We estimate the absolute magnitude of V4633 Sgr at maximum brightness, $M_{V,0}$, by two methods. First, we use the empirical maximum magnitude–rate of decline (MMRD) relation obeyed by novae. We use the linear MMRD relations for t_2 and t_3 derived by Downes & Duerbeck (2000) from an ensemble of 28 measured novae. Their relations yield for V4633 Sgr values of $M_{V,0} = -8.1 \pm 0.6$ and -7.9 ± 0.8 mag, respectively. Downes & Duerbeck (1981) also derived MMRD relations for t_2 and t_3 from 17 nova classified as B, C and D in the LC classification scheme of Duerbeck (1981). These relations yield for V4633 Sgr values of $M_{V,0} = -7.4 \pm 1.1$ and -7.2 ± 1.7 mag, respectively.

We can also estimate $M_{V,0}$ using the absolute magnitude 15 d after maximum, which appears to be independent of speed class (Warner 1995). Downes & Duerbeck (2000) derived from 28 objects a value of $M_{V,15} = -6.05 \pm 0.44$ mag. This value, together with our estimate of the visual magnitude of V4633 Sgr at maximum, $m_{V,0} = 7.7 \pm 0.1$ mag (Section 4.5.1), and with the value of $m_{V,15} = 9.45 \pm 0.06$ mag that was measured for V4633 Sgr at WO on JD 245 0912.51, yields $M_{V,0} = -7.8 \pm 0.5$ mag for the absolute magnitude of V4633 Sgr at maximum brightness.

We adopt the average of the above results, $M_{V,0} \approx -7.7$ mag, for the intrinsic magnitude at maximum.

Incorporating our estimations of the reddening, and the intrinsic and apparent maximum brightness of the nova into the distance modulus equation (Allen 1976), we derive a distance of 8.9 ± 2.5 kpc to V4633 Sgr, compatible with the estimation of Ikeda et al. (2000). We note that the derived distance to V4633 Sgr implies that it probably belongs to the population of ‘bulge’ novae. Indeed, the spectroscopic classification of V4633 Sgr as a Fe II nova, as well as its rate of decline, are characteristic of ‘bulge’ novae (Della Valle & Livio 1998).

5 SUMMARY

Three-year observations of V4633 Sgr revealed two photometric periodicities in the light curve of the nova. We interpret the shorter one, $P_2 = 3.014$ h, as the orbital period of the underlying binary system. The longer period, $P_1 = 3.08$ h, varied during 1998–2000 with $\dot{P}_1 = (-1.26 \pm 0.05) \times 10^{-6}$. The beat of the two periods, $P_3 = 5.06$ d, was probably present in the LC in 1999.

The period P_1 may be interpreted as a permanent superhump, or, alternatively, as the spin period of the white dwarf in a nearly synchronous magnetic system. V4633 Sgr would be a unique SH system, since its relative period excess is exceptionally small – ~ 2.5 per cent. This may imply an extremely low mass ratio. The characteristics of V4633 Sgr are also unique for the near-synchronous polar model.

Further photometric monitoring of V4633 Sgr in the next few years will probably allow us to determine the classification of the system, since the non-orbital period is expected to evolve differently in the two models. Radial velocity measurements should be done to confirm the orbital period. Time-resolved polarimetry and X-ray observations should be conducted to test the near-synchronous polar interpretation.

ACKNOWLEDGMENTS

We are grateful to Dina Prialnik for some very useful discussions. This research has made use of the VSNET data base. We thank Albert Jones for sending his visual estimates to us. Astronomy at the WO is supported by grants from the Israel Science Foundation. AR was supported by PPARC during most of the period during which this work was carried out, and is currently supported by the Australian Research Council.

REFERENCES

- Allen C. W., 1976, *Astrophysical Quantities*. Athlone Press, London
 Bonnet-Bidaud J. M., Mouchet M., 1987, *A&A*, 188, 89
 Brosch N., Goldberg Y., 1994, *MNRAS*, 268, L27
 Chochol D., Hric L., Urban Z., Komžik R., Grygar J., Papoušek J., 1993, *A&A*, 277, 103
 Della Valle M., Livio M., 1998, *ApJ*, 506, 818
 Della Valle M., Pizzella A., Bernardi M., 1998, *IAU Circ.*, 6848
 Downes R. A., Duerbeck H. W., 2000, *AJ*, 120, 2007
 Duerbeck H. W., 1981, *PASP*, 93, 165
 Efron B., Tibshirani R. J., 1993, *An Introduction to the Bootstrap*. Chapman & Hall, London
 Ferland G. J., 1977, *ApJ*, 215, 873
 Geckeler R. D., Staubert R., 1997, *A&A*, 325, 1070
 Hachisu I., Kato M., 2000, *ApJ*, 540, 447
 Hachisu I., Kato M., Kato T., Matsumoto K., Ken'ichi N., 2000, *ApJ*, 534, L189
 Howell S. B., Rappaport S., Politano M., 1997, *MNRAS*, 287, 929
 Ikeda Y., Kawabata K. S., Akitaya H., 2000, *A&A*, 355, 256
 Jones A. F., 1998, *IAU Circ.*, 6848
 Kaluzny J., Semeniuk I., 1987, *Acta Astron.*, 37, 349
 Kaspi S., Ibbetson P. A., Mashal E., Brosch N., 1995, *Wise Obs. Tech. Rep.*, No. 6
 Kaspi S., Smith P. S., Netzer H., Maoz D., Jannuzi B. T., Giveon U., 2000, *ApJ*, 533, 631
 Kato M., Hachisu I., 1994, *ApJ*, 437, 802
 Lance C. M., McCall M. L., Uomoto A. K., 1988, *ApJS*, 66, 151
 Leibowitz E. M., 1993, *ApJ*, 411, L29
 Leibowitz E. M., Ibbetson P., Ofek E. O., 1999, *Balt. Astron.*, 9, 403
 Liller W., 1998, *IAU Circ.*, 6846

Table A1 – continued

Liller W., Jones A. F., 1999, *Inf. Bull. Variable Stars*, 4664
 Lipkin Y., Leibowitz E. M., 2000, *IAU Circ.*, 7372
 Lipkin Y., Retter A., Leibowitz E. M., 1998, *IAU Circ.*, 6963
 Mason P. A., Ramsay G., Andronov I., Kolesnikov S., Shakhovskoy N., Pavlenko E., 1998, *MNRAS*, 295, 51
 Miller J. S., Mathews W. G., 1972, *ApJ*, 172, 593
 Mukai K., 1998, *ApJ*, 498, 394
 Neckel Th., Klare G., 1980, *A&AS*, 42, 251
 Netzer H. et al., 1996, *MNRAS*, 279, 429
 O'Donoghue D., Charles P. A., 1996, *MNRAS*, 282, 191
 Osaki Y., 1985, *A&A*, 144, 369
 Osaki Y., 1996, *PASP*, 108, 39
 Osterbrock D. E., 1989, *Astrophysics of Gaseous Nebulae and Active Galactic Nuclei*. University Science Books, Mill Valley, CA
 Patterson J., 1979, *ApJ*, 231, 789
 Patterson J., 1995, *PASP*, 107, 657
 Patterson J., 1998, *PASP*, 110, 1132
 Patterson J., 1999, in Mineshige S., Wheeler J. C., eds, *Disk Instabilities in Close Binary Systems: 25 Years of the Disk-Instability Model*. Universal Academy Press, Tokyo, p. 61
 Patterson J., Skillman D. R., 1994, *PASP*, 106, 1141
 Patterson J., Skillman D. R., Thorstensen J., Hellier C., 1995, *PASP*, 107, 307
 Prialnik D., 1986, *ApJ*, 310, 222
 Prialnik D., Kovetz A., 1995, *ApJ*, 445, 789
 Ramsay G., Buckley D. A. H., Cropper M., Harrop-Allin M. K., 1999, *MNRAS*, 303, 96
 Retter A., Naylor T., 2000, *MNRAS*, 319, 510
 Retter A., Leibowitz E. M., Kovo-Kariti O., 1998, *MNRAS*, 293, 145
 Retter A., Hellier C., Augusteijn T., Naylor T., Bembrick C., McCormick J., Velthuis F., 2001, *MNRAS*, submitted
 Rudy R. J., Lynch D. K., Mazuk S., Puetter R. C., Woodward C. E., 1999, *IAU Circ.*, 7259
 Rudy R. J., Lynch D. K., Mazuk S., Venturini C., Puetter R. C., Armstrong T., 2000, *IAU Circ.*, 7491
 Scargle J. D., 1982, *ApJ*, 263, 835
 Schmidt G. D., Stockman H. S., 2001, *ApJ*, 548, 410
 Schmidt G. D., Liebert J., Stockman H. S., 1995, *ApJ*, 441, 414
 Skiff B. A., 1998, *IAU Circ.*, 6851
 Skillman D. R., Patterson J., 1993, *ApJ*, 417, 298
 Skillman D. R., Harvey D., Patterson J., Vanmunster T., 1997, *PASP*, 109, 114
 Smith D. A., Dhillon V. S., 1998, *MNRAS*, 301, 767
 Stetson P. B., 1987, *PASP*, 99, 191
 Stockman H. S., Schmidt G. D., Lamb D. Q., 1988, *ApJ*, 332, 282
 Stolz B., Schoembs R., 1984, *A&A*, 132, 187
 van den Bergh S., Younger P. F., 1987, *A&AS*, 70, 125
 Warner B., 1995, *Cataclysmic Variable Stars*. Cambridge Univ. Press, Cambridge
 Whitford A. E., 1958, *AJ*, 63, 201
 Williams R. E., 1994, *ApJ*, 426, 279
 Williams R. E., Hamuy M., Phillips M. M., Heathcote S. R., Wells L., Navarrete M., 1991, *ApJ*, 376, 721
 Williams R. E., Phillips M. M., Hamuy M., 1994, *ApJS*, 90, 297

APPENDIX A: LOG OF OBSERVATIONS

Table A1. Log of observations.

UT Date	Time of start (HJD - 245 0900)	Run time (h)	Points per filter		
			I	V	B
980408	12.51	0.04	1	1	1
980409	13.51	2.3	569		
980412	16.51	2.1	272	2	
980413	17.50	2.4	163	164	
980420	24.50	2.1	104	99	

UT Date	Time of start (HJD - 245 0900)	Run time (h)	Points per filter		
			I	V	B
980509	43.47	0.7	43		
980511	45.44	3.6	214	168	
980512	46.41	1.3	89	88	
980607	72.35	5.5	493		
980608	73.35	5.5	284	280	1
980609	74.34	5.3	211	210	
980611	76.34	5.5	243	242	
980612	77.35	5.4	452		
980613	78.38	4.7	173		
980703	98.27	4.2	57	57	54
980704	99.28	4.2	45	45	45
980705	100.38	fosc			
980709	104.26	5.7	325		
980710	105.26	5.8	38	38	37
980711	106.24	4.2	38	38	37
980724	119.38	2.2	15	15	12
980729	124.34	2.2	16	15	15
980730	125.31	2.7	20	20	19
980803	129.36	1.9	15	15	15
980806	132.23	4.5	36	36	34
980807	133.23	4.4	30	30	30
980808	134.23	4.5	33	32	32
980809	135.25	4.0	30	29	29
980810	136.24	4.3	38	38	36
980811	137.28	2.5	17	17	17
980830	156.25	fosc			
980911	168.21	0.6	2	2	2
980913	170.21	0.7	3	2	2
980918	175.20	0.3	1	1	1
980919	176.20	0.3	2	1	1
980920	177.21	0.3	1	1	1
990418	387.57	0.1		1	
990425	394.46	3.3	24	22	21
990426	395.45	3.7	28	24	23
990427	396.45	3.6	28	23	23
990428	397.45	3.5	24	24	24
990429	398.44	2.9	19	19	18
990502	401.52	fosc			
990503	402.44	3.7	34	34	1
990518	417.39	4.8	35	32	31
990519	418.53	1.0	7	7	7
990520	419.53	1.0	7	7	7
990523	422.37	5.1	35	33	32
990524	423.37	5.2	39	33	32
990525	424.36	5.3	39	34	31
990526	425.41	4.2	136	1	1
990528	427.35	4.2	40	4	2
990529	428.35	5.6	50	42	3
990615	445.44	0.02	1		
990619	449.40	0.7	5	5	5
990621	451.41	0.1	1	1	1
990622	452.43	0.1	1	1	1
990624	454.28	6.7	44	27	18
990625	455.28	6.6	52	43	
990626	456.27	6.9	74	43	
990630	460.27	6.7	71	56	
990701	461.27	6.6	73	63	
990702	462.28	6.4	51	44	37

Table A1 – continued

UT Date	Time of start (HJD – 245 0900)	Run time (h)	Points per filter		
			I	V	B
990703	463.26	6.8	109	97	0
990704	464.26	6.8	108	101	0
990705	465.25	6.6	56	44	32
990706	466.29	fosc			
990707	467.24	7.1	117	101	
990729	489.26	5.0	241		
990730	490.22	5.8	156		
990731	491.22	56.0	154		
990801	492.22	6.1	155		
990802	493.22	0.3	6		
990803	494.23	4.0	101		
000327	731.60	0.2	1	1	1
000416	751.47	2.7	26		
000417	752.46	3.4	44	1	2
000421	756.45	1.8	24		
000422	757.46	3.1	2	29	
000511	776.41	4.3	28	28	1
000513	778.41	3.8	29	28	1
000514	779.44	3.1	27	24	1
000515	780.43	2.6	22	22	2
000720	846.35	2.6	43		
000721	847.23	6.2	111		
000722	848.23	6.2	111		
000723	849.23	6.1	109		
000727	853.37	0.9	16		
000728	854.31	2.6	48		
000729	855.30	2.6	42		
000803	860.31	2.1	33		
000804	861.34	2.4	42		
000804	861.24	2.5	(529 ‘clear’)		
000805	862.24	5.2	94		
000806	863.22	5.5	93		
000817	874.27	2.9	40		
000818	875.22	4.2	72		
000819	876.21	4.6	84		
000820	877.21	4.9	629		
000821	878.21	4.8	686		
000822	879.21	2.1	29		

This paper has been typeset from a $\text{\TeX}/\text{\LaTeX}$ file prepared by the author.